J. Basic. Appl. Sci. Res., 2(1)433-448, 2012

ISSN 2090-4304
Journal of Basic and Applied Scientific Research
www.textroad.com

Signal Processing Algorithms in Ground Surveillance Pulse Doppler Radar Designed for Clutter Suppression

[1]Naser Parhizgar , [2]Abbas Sheikhi, [1]Zeinab Khodkar

[1]Department of Electrical Engineering, Science and Research Branch, Islamic Azad University, Fars, Iran.
[2]Faculty of Electrical and Computer Engineering, Department of Communication, Engineering Shiraz University, Shiraz, Iran.

ABSTRACT

The aim of this paper is to design an efficient and realizable detection algorithm for ground surveillance pulse Doppler radar. In order to attain this purpose, an efficient approach is to use Doppler filters bank based upon spectral estimation. Parametric and non-parametric spectral estimation techniques in the context of surveillance pulsed Doppler radar clutter suppression is proposed in the paper. The research results are declared for 4 different wind conditions. Furthermore two algorithms (i.e. filter slope CFAR and filter CFAR) are presented to suppress the clutter and are compared with slope CFAR algorithm. Also AR Yule-walker method is applied to spectral estimation. This method is based upon linear direct relationships between signal autocorrelation and AR parameters. Moreover an algorithm which combines parametric and non-parametric techniques is suggested and explained in a separate section. The aforementioned algorithm is also depicted in detail. In this algorithm, clutter spectrum is estimated by using AR Yule-Walker method and arrival signal spectrum is estimated by using non-parametric techniques. Finally, non-parametric technique PD curves (i.e. probability of detection curves) are simulated with respect to SCR for each wind condition and simulation results are depicted and compared.
KEY WORDS: Slope CFAR, filter slope CFAR, filter CFAR, AR-CFAR, Yule-Walker.

1. INTRODUCTION

The most significant problem with target detection is unwanted echoes of the objects other than target such as mountain, sea, land, trees, rain, etc. These undesired echoes are referred to as "clutter", which affect target detection. The aim of this paper is to suppress the clutter in received signals. Echoes which are reflected from target are mixed up and corrupted with clutter before they arrive to the radar. It should be noted in pulse Doppler radar that target echoes are weaker than clutter. Therefore efficient techniques are required for moving target detection in presence of strong clutter. Nowadays, cancellers, Doppler filters, Doppler filters bank and adaptive detectors are the most commonly used methods. Signal detection based on spectral estimation which performs by using Doppler filters bank is the best choice in this kind of radar application, due to the fact that although detector should be adapted with the environment, clutter spectrum is fluctuating. The main problem with filters bank is obviously high computational burden of this kind of filters, so efficient techniques should be used for implementing Doppler filters banks.

The aim of spectral estimation techniques is to deduce the Power of Spectral Density (PSD) from a finite output data sequence of process of interest. The issue has been significantly studied over the years. Therefore, so many techniques have been derived to estimate spectrum of the signal. In order to achieve an efficient algorithm, several spectral estimation techniques are designed here and all of them are simulated through radar base band signal simulator and results are presented in the sequel. Arrival signal spectrum should be estimated before being detected. Hereupon spectral estimation which is referred to as achieving arrival frequency content should be carried out. This estimation technique is classified in two main categories: parametric techniques and non-parametric techniques, which are expatiated in the paper. The main difference between parametric spectral estimation techniques and non-parametric techniques is the fact that in parametric techniques, a model should be supposed for the signal spectrum contemplating signal nature, but non-parametric spectral estimation techniques neglect intrinsic properties of the signal. Although parametric techniques result more accurate estimates of short-term power spectrums, they have usually more computational complexity. If there is significant number of arrival snapshots, aforementioned techniques offer quasi-performance. Autoregressive modeling is widely used in many radar systems to suppress clutter effect. In order to implement AR detection, first the received signal should be modeled, and unknown parameters could be estimated using arrival snapshots thereafter.

Algorithms proposed in the paper are studied through computer simulation and results are plotted in figures. In general, parametric methods with accurate models which are suited for the given application are capable to provide more accurate and robust estimates of the short-term power spectrum. This article offers design of techniques which are mentioned above and delineates corresponding simulation results by radar base band signal simulator. The presented algorithm is classified into three general categories below: (1) Non-

Corresponding Author: Naser Parhizgar, Department of Electrical Engineering, Science and Research Branch, Islamic Azad University, Fars, Iran. E-mail: parhizkar@fsriau.ac.ir

Parametric spectral estimation techniques, (2) Parametric spectral estimation techniques,(3) use of both techniques together.

2. NON-PARAMETRIC SPECTRAL ESTIMATION TECHNIQUES

In these techniques the frequency domain is first divided into several sub-bands as filters, then signal is applied to these filters. Each filter corresponds to one of the aforementioned sub-bands. We can approximate the spectrum shape using measured output power of these filters, thereafter. A common approach to design and implement these filters is to use methods based on filters bank. Filters bank is referred to as the arrays of band-pass filters which cause separation of arrival signal into several components; each is corresponding to a unique frequency sub-band of the original signal. Generally in non-parametric techniques, signal is applied to narrow bandpass filters which probe whole frequency domain area of interest, and then filters output power is utilized as spectral nature of the arrival signal. This section introduces three non-parametric spectral estimation algorithms which are designed based upon Fast Fourier Transform for ground surveillance radar. Each of them is expatiated in separate sub-sections. The explanation is provided using block diagrams and simulations. Finally, best approaches are introduced and compared with other methods which are investigated in the article.

2.1. SLOPE CFAR ALGORITHM

The structure of the algorithm is depicted in figure 2 and each block operation is explained in detail in the following lines:

FFT block: first a hamming window is required then N-point FFTs should be applied. The main problem with FFT is the fact that computational complexity of the approach increases as the number of FFT points increases and accuracy reduces as number of points decreases.

ABS block: absolute values of previous block output data are computed here using relationship $\left\{(\mathrm{Re}al)^2+(\mathrm{Im}ag)^2\right\}^{1/2}$.A good approximation of them also could be achieved by relationship $|\mathrm{Re}al|+|\mathrm{Im}ag|$.

IIR filter block: in order to smooth the ripples of spectrum there is necessity to use a low-pass filter. The following relationships achieve z transfer function of the filter which is indicated figure 1 by block diagram.

$$y(n)=ay(n-1)+(1-a)x(n) \tag{1}$$

$$h(n)=a^nU(n)\times(1-a) \tag{2}$$

$$H(z)=\frac{1-a}{1-az^{-1}} \tag{3}$$

The output W(n) is delineated in figure (3) for worst wind condition (i.e. gale force), and for a target with 0.28 m^2 radar cross section and 300 Hz Doppler frequency.

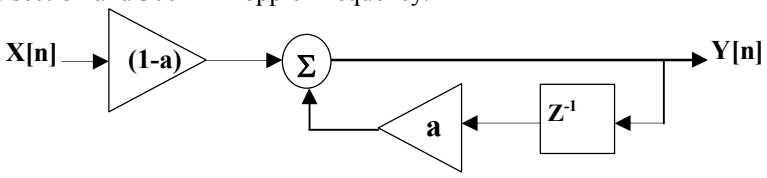

FIGURE 1. IIR Filter Block Diagram

As it is obvious in figure 1, block diagram is handled to depict what IIR filter exactly perform.

Noise level estimation block: Noise level is referred to as spectral data average. The output data of IIR filter block which is represented as Y[n] in figure 1 helps us to estimate noise level.

4 wind conditions block: this block contains slope parameters which are indicated in table below. Table 1 allocates values to each wind condition which depend on user choice. Slope parameters specify adaptive threshold level. These slope values should be transmitted to adaptive threshold block and must be inserted to the equation 4 which is written in the following lines.

TABLE 1. Slope Values Which Depend on Wind Conditions

Wind Condition	Slope Value
Light air	0.4
Breezy	0.45
Windy	0.55
Gale Force	0.65

Adaptive threshold block: this block eliminates clutter effect. Filter output is represented by W in figure 2. Clearly targets which have frequencies less than 50 Hz are often ignored, so clutter spectrum should be approximated for the frequencies upper than 50 Hz, using the relation below [5]

$$C(j+4) = W(4) \times (slope)^{j} \qquad for \quad j = 0 : till - 4 \tag{4}$$

$$till = \frac{\log(1.1 \times N/W(4))}{\log(slope)} + 4 \tag{5}$$

Where C(.) represents clutter spectrum and should be subtracted from W(.). Each type of clutter spectrum is corresponding to the only one of the slope parameters values which are listed in table 1. Recall that clutter spectrum is exponential therefore C should be neglected for frequencies greater than an upper bound which is computed in adaptive threshold block and is represented by $till$ in equation 5.

Equation 4 is accurate when C>N or C=1.1N. The output of this block is $T(n) = W(n) - C(n)$ and is indicated in figure 3 for worst wind conditions (i.e. gale force), and for a target with 0.28 square meters radar cross section and 300 Hz Doppler frequency.

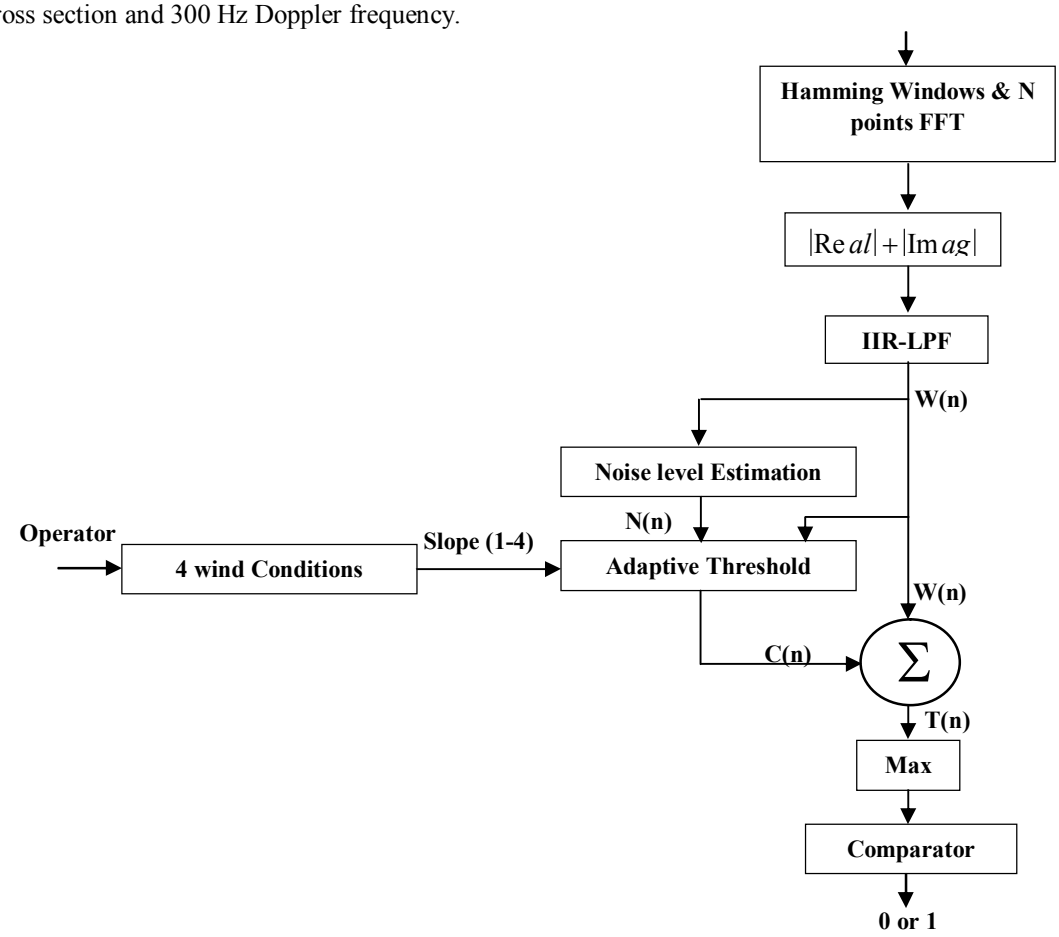

FIGURE 2. Slope CFAR Block Diagram Algorithm.

Max block: This block finds and saves maximum value of T.

Comparator block: Previous block output data and threshold level are compared here. If data is more than threshold level the output is 1 otherwise it is 0.

A signal is applied to the input of block diagram of figure 2 in software environment. Simulation results are shown in figure 3 for gale force clutter and for a target with RCS=0.28 m^2 and F_d=300 Hz. The curve, shown at the top of figure 3, contains signal and clutter mixed together. The second curve illustrates clutter spectrum which is estimated using slope CFAR algorithm and third curve at the bottom of figure 3 represents target echo due to subtraction of two previous curves. Also threshold level is illustrated here.

Slope parameter determines the slope of the exponential clutter spectrum and noise level estimation indicates the starting amplitude. Plotting the curves could be started by using these two parameters.

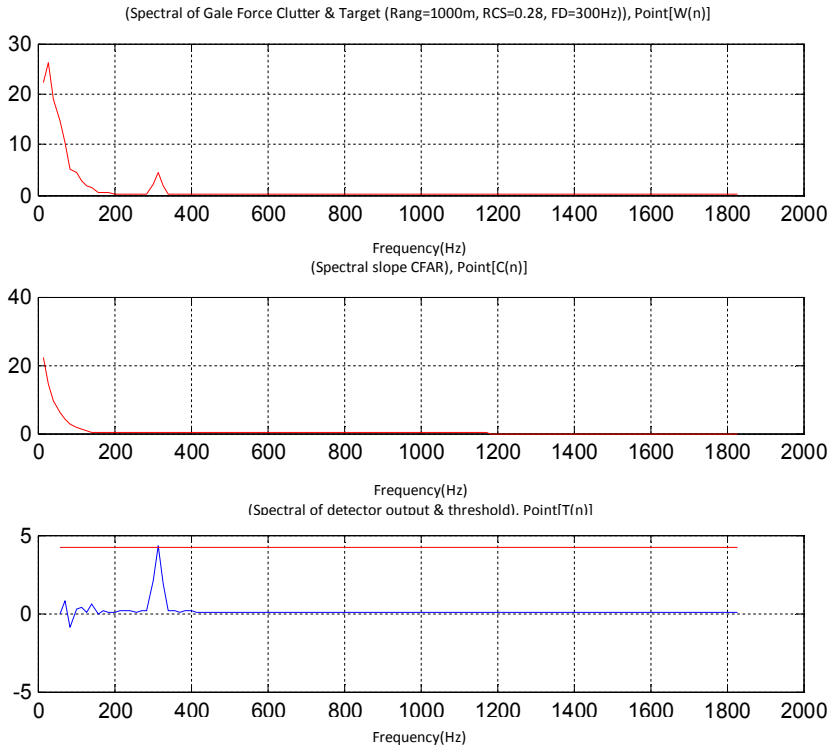

FIGURE 3. Outputs of the Different Parts of Slope CFAR Algorithm for Gale Force Clutter and for a Target with RCS=0.28 m^2 and F_d=300 Hz.

2.2. FILTER SLOPE CFAR ALGORITHM

The algorithm structure is depicted in figure 4. Outputs of Each block are investigated in the following.

3 Stages Cascade Transposed IIR-LPF Block: This block represents 3 stages IIR filters which could be realized with transposed structure. In order to alleviate sensitivity and instability of the filter with respect to quantization error, coefficients of high-order filters (i.e. greater than 2), are implemented. The transfer function of each stage is

$$H(z)=\frac{b_0+b_1z^{-1}+b_2Z^{-2}}{L-a_1z^{-1}-a_2z^{-2}}=\frac{y(z)}{x(z)} \tag{6}$$

Therefore differential equation of stages could be written as

$$LY(n)=b_0X(n)+b_1X(n-1)+b_2X(n-2)+a_1Y(n-1)+a_2Y(n-2) \tag{7}$$

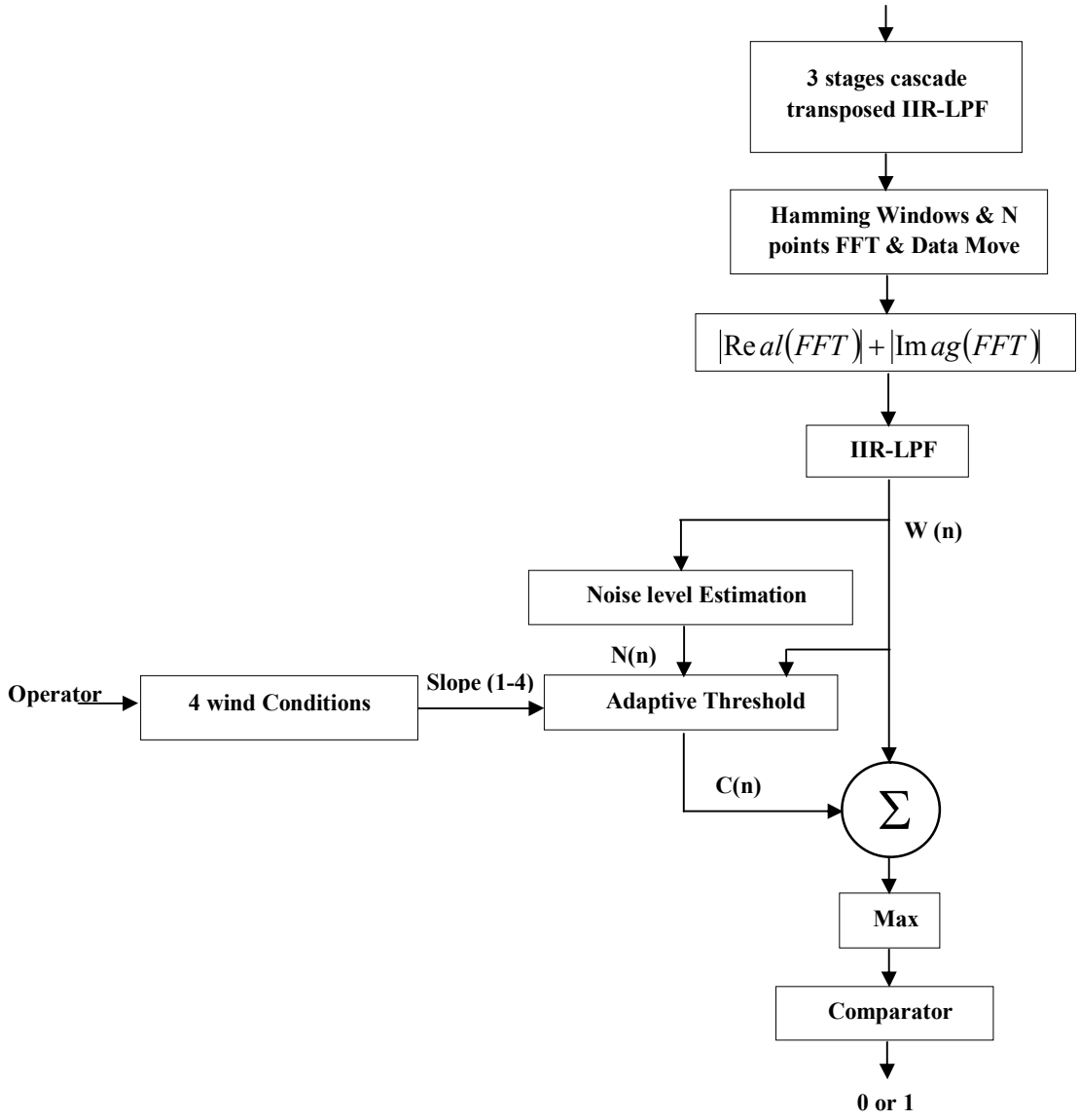

FIGURE 4. Filter CFAR Detector Structure

The signal flow graph which depicts transposed Direct-Form-II realization of cascaded second-order stages is delineated in figure 5. Other blocks in the diagram perform operations similarly to operations which have already been described for slope CFAR algorithm.

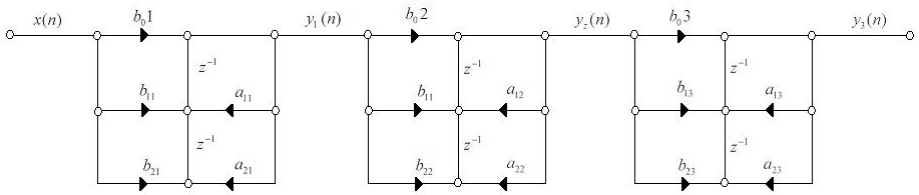

FIGURE 5. Transposed Direct-Form-II for 6th Order Filter

Simulation results are indicated in figure 6 for worst wind conditions (i.e. gale force), and for a target with 0.18 square meters RCS and 300 Hz Doppler frequency.

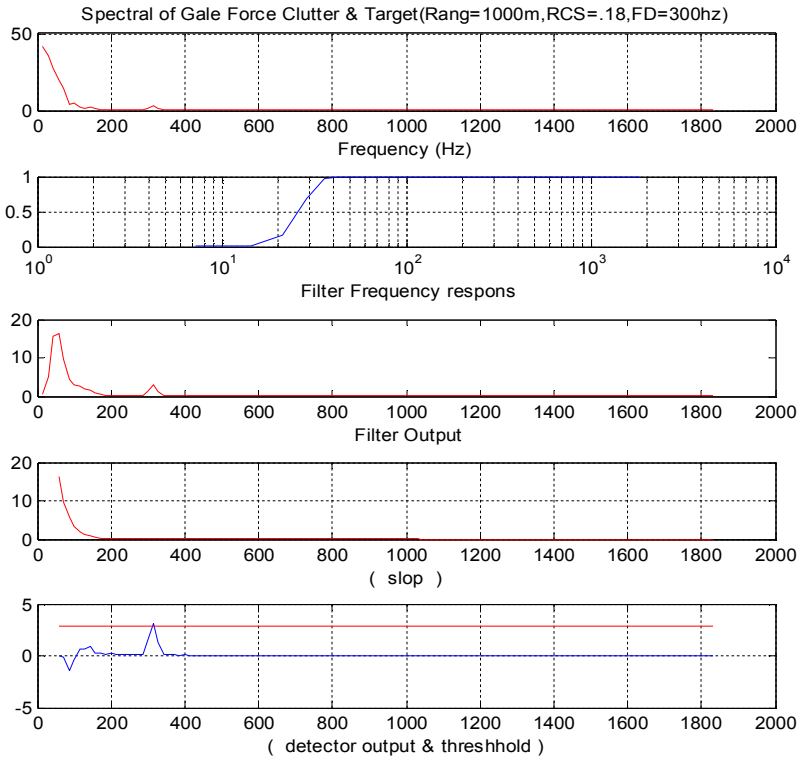

FIGURE 6. Outputs of Different Parts of Filter Slope CFAR Algorithm for Gale Force Clutter and for a Target with RCS=0.18m^2 and F_d=300 Hz.

2.3. FILTER CFAR ALGORITHM

The block diagram of the algorithm is illustrated in figure 7. Obviously, 3 Stages cascaded Transposed form of IIR-HPF which contains second- order IIR-HP filters can eliminate clutter effect. Filter coefficients are implemented as second order cascaded stages, to alleviate sensitivity and instability of the filter with respect to the quantization error. The filter frequency response shown in figure 8 indicates the fact that spectrum is attenuated by almost 60 dB between 0 to 40 Hz. This filter limits clutter between 0 to 40 Hz and allows Doppler frequencies between 60 Hz to 183 Hz. Therefore Minimum Doppler frequency of interest (i.e. 60 Hz), could pass through the filter.

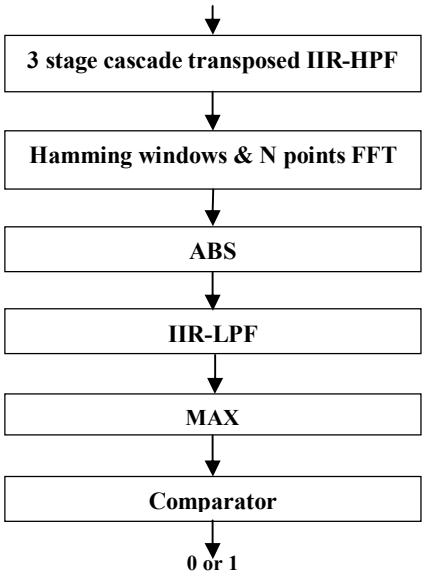

FIGURE 7. Block Diagram of Filter CFAR Algorithm

Then the output is transmitted into Windows and FFT block and passes through Doppler filters bank. Absolute value of the signal is also computed in ABS block thereafter.

In order to smooth the fast ripples, signal should be transmitted to the IIR-LPF block, which is a first order IIR low pass filter. Finally, after delineating maximum output of the filters bank by using MAX block, signal is inserted into the Comparator block to be compared with threshold level and the result becomes zero or one as output.

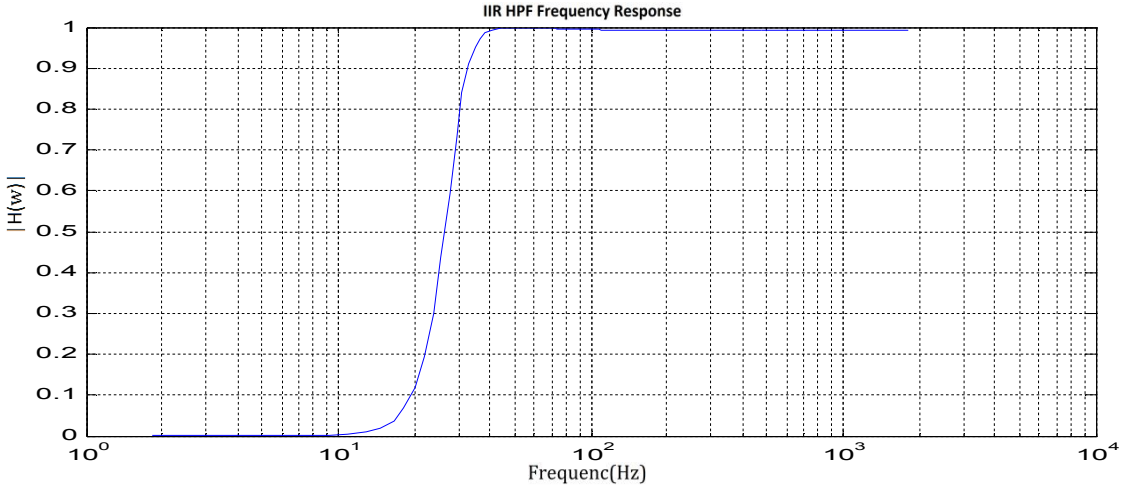

FIGURE 8. IIR High-Pass Filter Frequency Response

3. PARAMETRIC SPECTRAL ESTIMATION TECHNIQUES

In these methods, spectral estimation is based upon signal Autoregressive model. Thereby these techniques are referred to as parametric techniques. Parametric techniques are contemplated here for model fractional spectrums (ARMA). The main effort is to accord fractional spectrum model with the arrival data.

As mentioned above, the main difference between non-parametric spectral estimation technique and parametric technique is the fact that in parametric methods, a model should be supposed for the signal spectrum, as the signal satisfies the model but non-parametric techniques neglect intrinsic properties of the signal. In other words parametric methods obtain spectral properties of the signal of interest by estimating its parameters.

3.1. AR MODEL

Autoregressive or whole pole model is a modeling technique with a large range of practically applications. AR model is significantly used to describe very narrow pick spectrums. This is an extremely important advantage due to the several practically usages of narrow band signals. Parameters estimations could be obtained by solving a linear equations set. It should be noted here that stability of estimated AR coefficients is guaranteed.

AR(p) indicates autocorrelation of autoregressive model of order p. The AR(p) model can be written as [1],[12].

$$X_t = \sum_{i=1}^{p} a_i X_{t-i} + \sigma_t^2 \tag{8}$$

Where, $a_1, \ldots, a_p$ are parameters of the model and σ_t represents white noise.

In this paper, in order to perform AR spectral estimation, Yule-Walker method is applied which is based on linear relationships between signal autocorrelation and AR parameters directly.

3.2. AR-CFAR ALGORITHM

As it is evident, ground clutter spectrum contains a narrow sharp pick and a wide vast vale. This clutter spectrum is significantly similarly to the AR model. AR- Constant False Alarm Rate (AR-CFAR) detector is designed here to estimate clutter spectrum using Yule-walker method. Detector algorithm is illustrated in figure 9 and outputs of different parts of the algorithm is indicated in figure 10 for worst wind condition (i.e. gale force), and for a target with 0.28 square meters RCS and 300 Hz Doppler frequency.

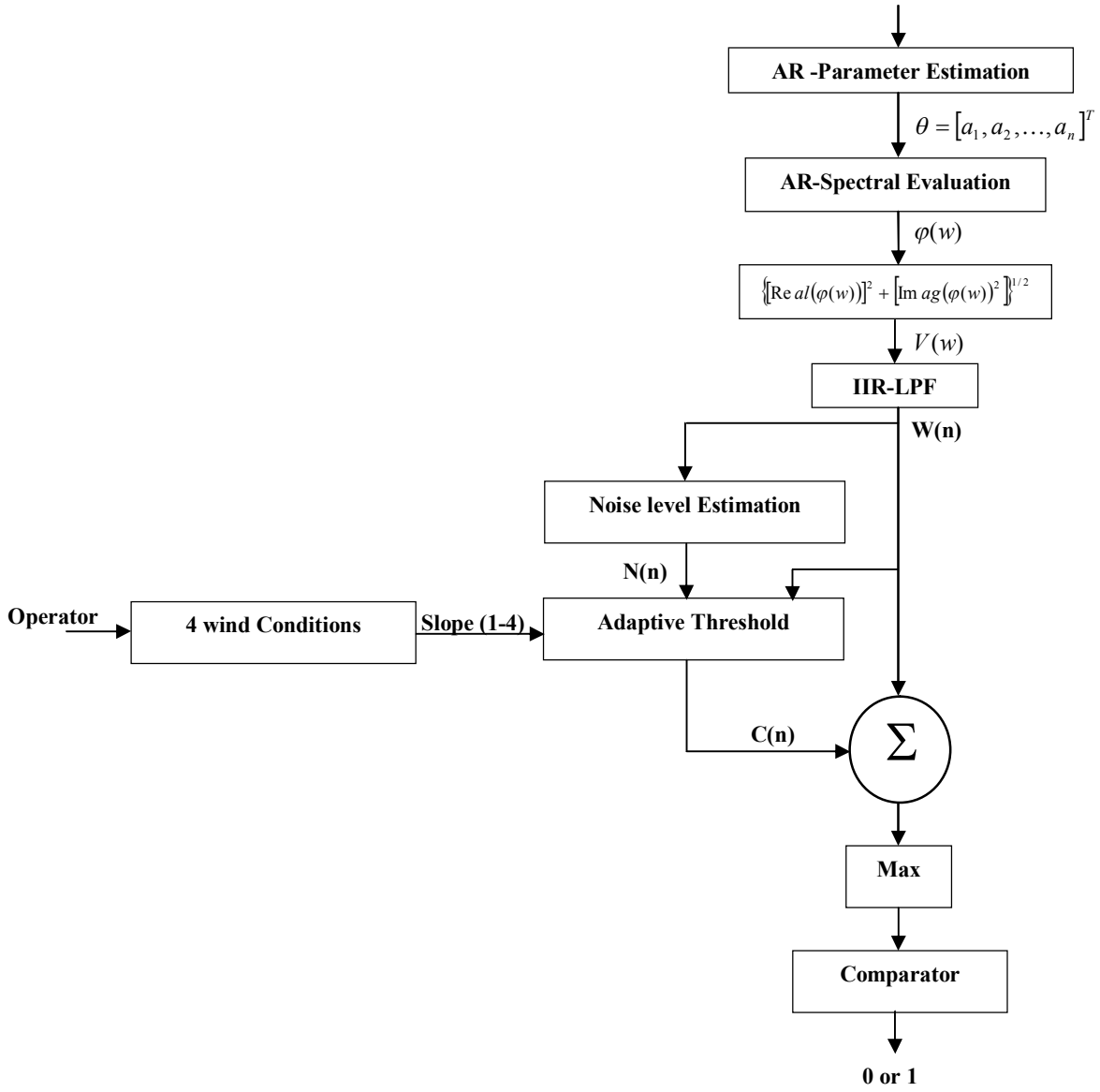

FIGURE 9. AR-CFAR Detection Algorithm Block Diagram

First in AR-parameter estimation block a hamming window is applied to the signal then signal parameters (i.e. $\theta = [a_1, a_2, \ldots, a_n]^T$) and σ^2 are evaluated using Yule-walker method. AR-Spectral Evaluation block achieves signal spectrum estimation based upon AR model. Absolute value of this block output could be achieved in ABS block thereafter. As described before, a first order IIR-LPF omits ripples. Finally, after delineating maximum output value of the filter bank, signal is inserted into the comparator block and is compared with threshold level.

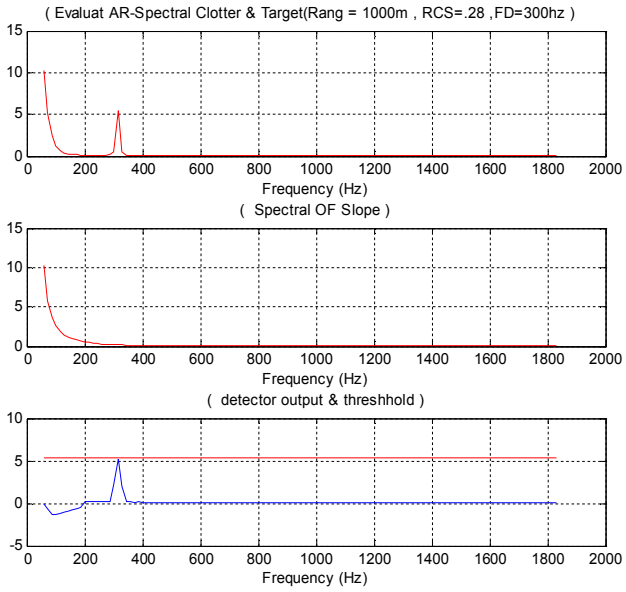

FIGURE 10. Outputs of Different Parts of AR-CFAR Algorithm for Gale Force and for a Target with RCS=0.28 m^2 and F_d=300 Hz.

3.3. YULE-WALKER TECHNIQUE FOR AR-SPECTRAL ESTIMATION

This approach focuses on the AR parameters estimation using Yule-walker technique.

In order to perform AR algorithm a white noise should be applied to a whole pole filter with the following transfer function

$$H(z)=\frac{1}{1-a_1 z^{-1}-\cdots-a_n z^{-n}} \tag{9}$$

The relationship between autocorrelation coefficients and AR model coefficients is

$$\begin{bmatrix} r(0) & r(-1) & \cdots & r(-n) \\ r(1) & r(0) & \cdots & \cdots \\ \vdots & \vdots & \ddots & \vdots \\ r(n) & r(n-1) & \cdots & r(0) \end{bmatrix} \times \begin{bmatrix} 1 \\ a_1 \\ \vdots \\ a_n \end{bmatrix} = \begin{bmatrix} \sigma^2 \\ 0 \\ \vdots \\ 0 \end{bmatrix} \tag{10}$$

The aforementioned equations are referred to as Yule-walker equations or normal equations. Suppose that $\{\hat{r}(k)\}_{k=0}^{n}$ is known, so we can write

$$\begin{bmatrix} r(1) \\ \vdots \\ r(n) \end{bmatrix} + \begin{bmatrix} r(0) & \cdots & r(-n+1) \\ \vdots & \ddots & \vdots \\ r(n-1) & \cdots & r(0) \end{bmatrix} \times \begin{bmatrix} a_1 \\ \vdots \\ a_n \end{bmatrix} = \begin{bmatrix} 0 \\ \vdots \\ 0 \end{bmatrix} \tag{11}$$

Or

$$r_n + R_n \theta = 0 \tag{12}$$

Where

$$\theta = [a_1, \ldots, a_n]^T \tag{13}$$

In order to calculate aforementioned relationships, suppose that

$$\theta = -R_n^{-1} r_n \tag{14}$$

σ^2 can be achieved from first row of the matrix in equation 10, by computing θ.

Yule-walker method uses equation 10 directly to perform AR spectral estimation. First; autocorrelation snapshots $\{r(k)\}_{k=0}^{n}$ for data $\{y(t)\}_{t=1}^{N}$ should be obtained and then should be inserted into equation 10. The

equation could be solved thereafter in order to achieve $\hat{\theta}$ and σ^2. The result concluded by these finite snapshots is similar to the case that all of autocorrelation snapshots are available.

4. USE OF BOTH PARAMETRIC AND NON-PARAMETRIC TECHNIQUES

The approach proposed here, offers a mixture of FFT based parametric and non-parametric techniques described above. Note that arrival signal contains clutter and target echoes mixed together. Therefore in order to reject clutter effect, clutter spectrum should be achieved first, then subtracting it from arrival spectrum yields target echo spectrum. The method presented here estimates clutter spectrum using AR model and Yule-walker method and also achieves signal spectrum by FFT based non-parametric technique. Then subtracts clutter from signal and eliminates clutter effect.

4.1. ADAPTIVE CFAR ALGORITHM

The structure of this algorithm is indicated in figure 11 and operations of each block are introduced in the following. The approach uses both FFT based parametric and non-parametric techniques to eliminate power spectrum of clutter from received signal. Outputs of different parts of algorithm are simulated for worst wind condition, (i.e. gale force), for a target with 0.28 m^2 RCS and 300 Hz Doppler frequency through computer and results are illustrated in figure 12.

Hamming windows block: this block decreases side lobe level.

Noise level estimation block: W and IIR low pass filter outputs are averaged here and considered as noise.

AR-parameter estimator block: Signal parameters (i.e. $\theta = [a_1, a_2, \ldots, a_n]^T$ and σ^2), are obtained here by using Yule-Walker method.

AR-spectral evaluation block: Model-based clutter spectrum with N-points accuracy and corresponding parameters (i.e. θ and σ^2), could be obtained in this part of algorithm.

ABS (2) block: Absolute value of output data of the AR-spectral estimation block could be computed here by using relationship $\{[\text{Real}\ (\varphi_w)]^2 + [\text{Imag}\ (\varphi_w)]^2\}^{1/2}$.

Adaptive threshold block: this block eliminates clutter effect. Note that IIR-LPF (2) output which is indicated by K(n) operates as slope parameter. C(n) represents estimated clutter spectrum and should be subtracted from signal W(n). So the output of this block is T=W-C and is accurate when C>N or C=1.1N. As mentioned above clutter spectrum is exponential, therefore C should be neglected for high frequencies.

Max block: this block finds maximum value of T and saves it.

Comparator block: this block represents comparison between maximum value of T and threshold level. If data is more than threshold level the output is 1 otherwise it is zero.

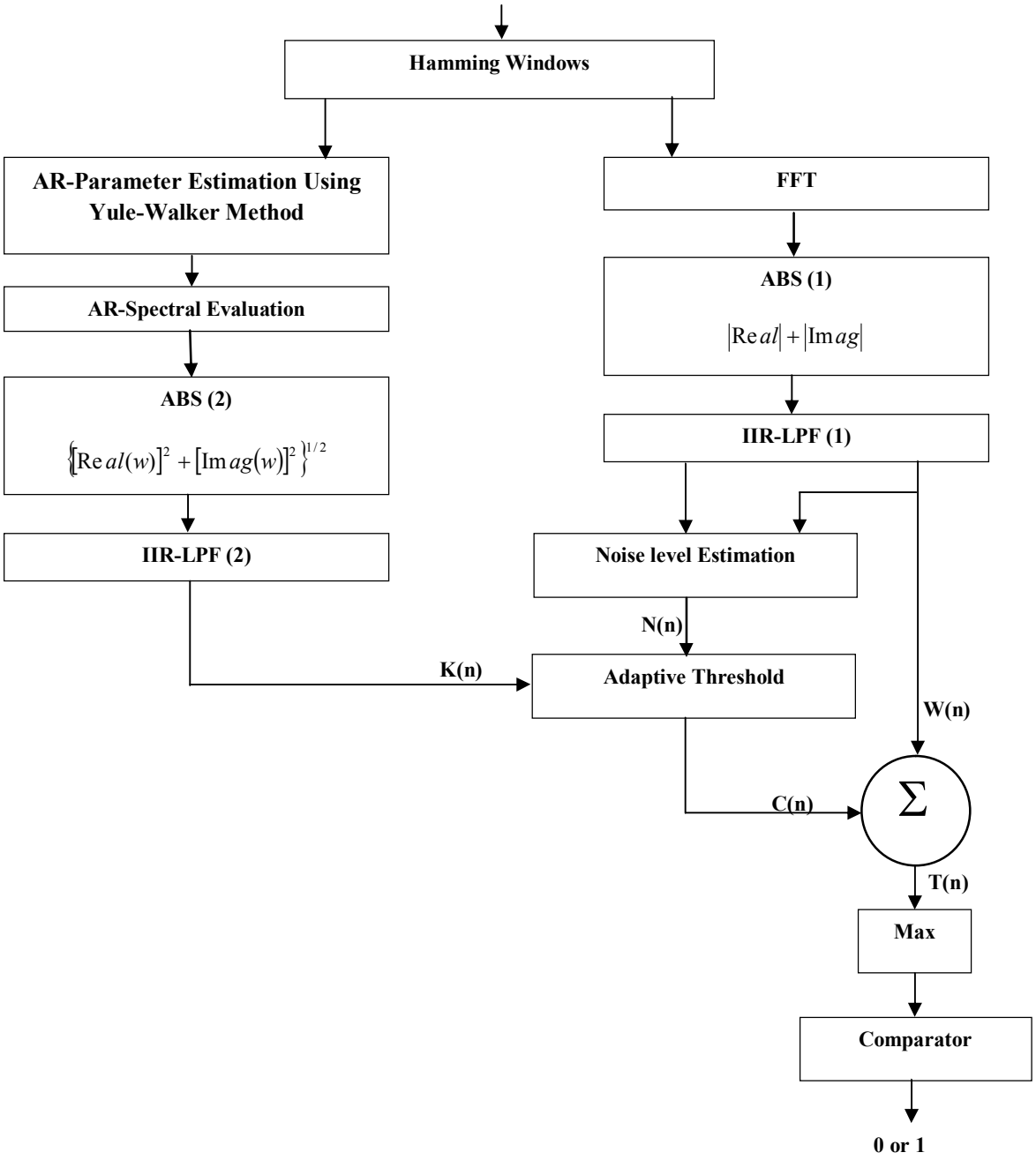

FIGURE 11 Adaptive CFAR Detector

Simulation results for a signal of interest which is inserted into suggested adaptive CFAR detector, is depicted in figure 14 for gale force clutter and a target with RCS=0.28 m^2 and F_d =300Hz.

5. SURVEY 0N DETECTORS QUALITY

This section involves simulation results of algorithms proposed in previous sections. A base band signal is supposed as input in simulator environment and results are plotted as Probability of Detection curves (PD) with respect to SCR for different conditions in figure 13 to 27. In order to compare performance of detectors, 16 states are listed in Table 2. The table indicates four different states for wind conditions which are considered in simulations and shows 16 different states which depend on target distance from radar and Doppler frequencies corresponding to the target radial velocity.

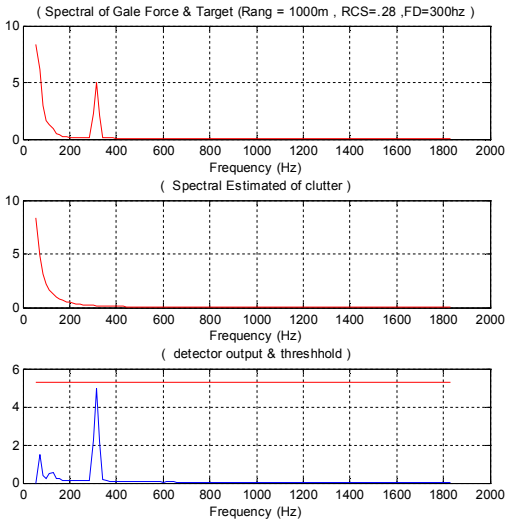

FIGURE 12. Outputs of Different Parts of Adaptive CFAR Algorithm for Gale Force Clutter and for a Target with RCS=0.28 m^2 and F_d =300 Hz.

TABLE 2. Different States Which are Assumed in Simulation Analysis

State	Clutter Type	Target distant	Target Doppler
1	First	Near	60 Hz
2	First	Far	60 Hz
3	First	Near	300 Hz
4	First	Far	300 Hz
5	Second	Near	60 Hz
6	Second	Far	60 Hz
7	Second	Near	300 Hz
8	Second	Far	300 Hz
9	Third	Near	60 Hz
10	Third	Far	60 Hz
11	Third	Near	300 Hz
12	Third	Far	300 Hz
13	Fourth	Near	60 Hz
14	Fourth	Far	60 Hz
15	Fourth	Near	300 Hz
16	Fourth	Far	300 Hz

5.1. FIRST STATE

As it is depicted in table 1, first type of clutter is referred to as light air which slope parameter is 0.4. Target simulated here is 1000 meters far from radar and its RCS is altered between $1\times10^{-2}m^2-5\times10^{-2}m^2$. Wind is supposed light air and PD curves are plotted with respect to the SCR for F_d=60 Hz and P_{FA}=10^{-4}. The results are shown in figure 13.

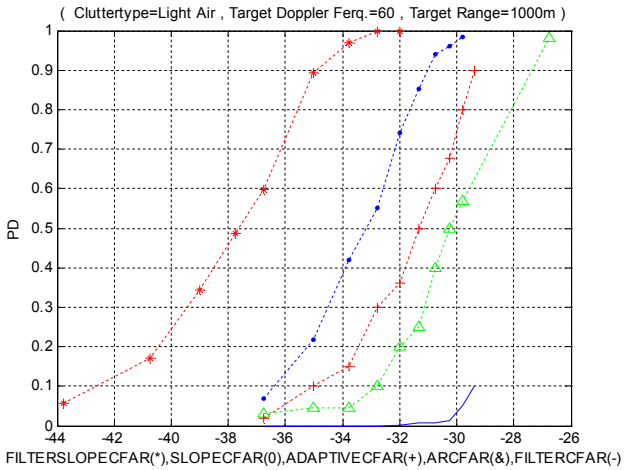

FIGURE 13. ROC Curve for First State

As it is obvious in figure 13, filter slope CFAR algorithm has high probability of detection versus less SCR. Slope CFAR shows a tradeoff between PD and SCR and shows better performance than AR-CFAR and Filter-CFAR.

Clearly, Filter-CFAR and AR-CFAR algorithms are weaker than the others. Comparison between aforementioned algorithms, (i.e. filter slope CFAR, slope CFAR and adaptive CFAR) for each wind condition specifies the algorithm which gives us the best performance.

5.2. FIFTH STATE

5th state in table 2 which is corresponding to the second type of clutter has slope parameter 0.45. Target simulated here is 1000 meters far from radar and its RCS is altered between $5\times10^{-2}m^2 - 4.5\times10^{-1}m^2$. Wind is supposed breezy and PD curves are drawn with respect to the SCR for F_d=60 Hz and P_{FA}=10^{-4}. Simulation results in figure 14 show the fact that adaptive CFAR and slope CFAR have poor performance but filter slope CFAR offers better results.

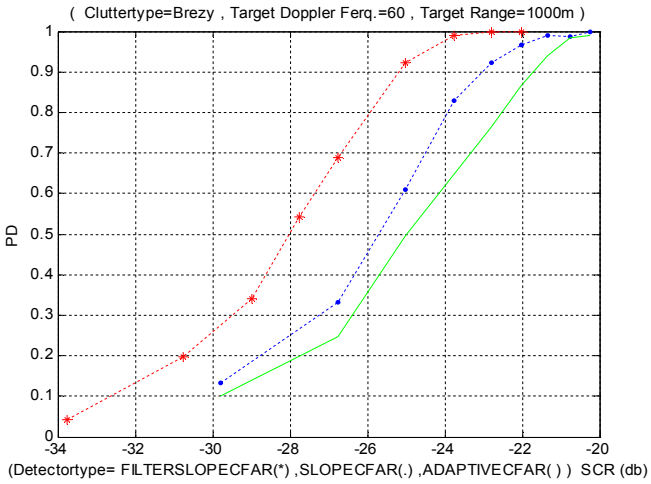

FIGURE 14. ROC Curve for 5th State

5.3. TENTH STATE

Clutter effect, caused by windy condition, is simulated here and its slope parameter is supposed 0.55. Target which is simulated here is 20000 meters far from radar and its RCS is altered between $1\times10^{-3}m^2 - 9\times10^{-3}m^2$. Target location is supposed far and PD curves are plotted with respect to the SCR for F_d =300 Hz and $P_{FA} = 10^{-4}$. The result is shown in figure 15.

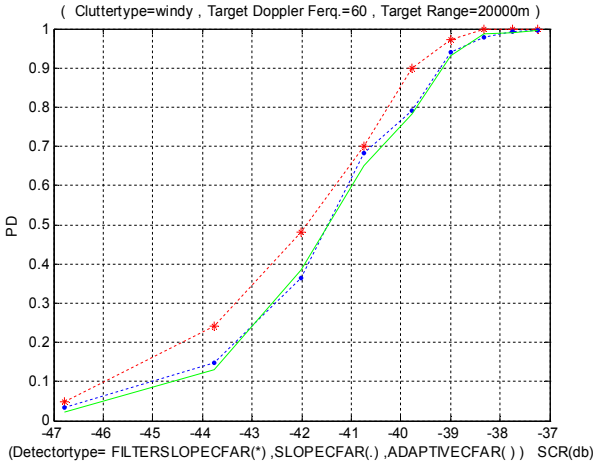

FIGURE 15. ROC Curve for 10th State

Figure 15 illustrates simulation results for clutter effect which is caused by windy air. As it is obvious slope CFAR and adaptive CFAR has quasi-performance but Filter Slope CFAR offers better PD.

5.4. FOURTEENTH STATE

Clutter effect which is caused by gale force condition is simulated here and its slope parameter is supposed 0.65. Target simulated here is 20000 meters far from radar and its RCS is altered between

$1\times10^{-3}m^2 - 9\times10^{-3}m^2$. Target location is supposed far and PD curves are plotted through simulation with respect to the SCR for F_d=60Hz and $P_{FA}=10^{-4}$. The result is shown in figure 16.

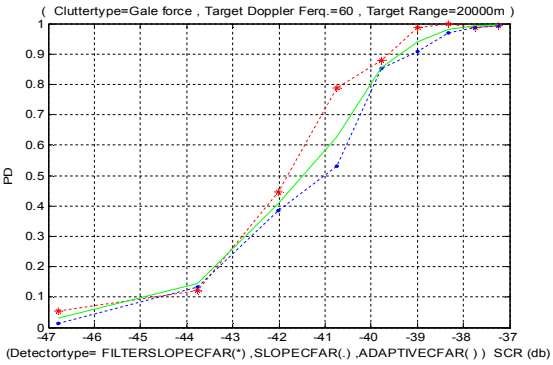

FIGURE 16. ROC Curve for State 14

Figure 16 illustrates simulation results for clutter effect which is caused by worst wind condition with slope parameter 0.65. As it is obvious, although three algorithms have quasi-performance for SCR less than -42 dB, filter slope CFAR has better PD than both CFAR and adaptive CFAR for SCR more than -42 dB.

In general the Comparison between figures 13 to 27 proves that filter slope CFAR is the best one.

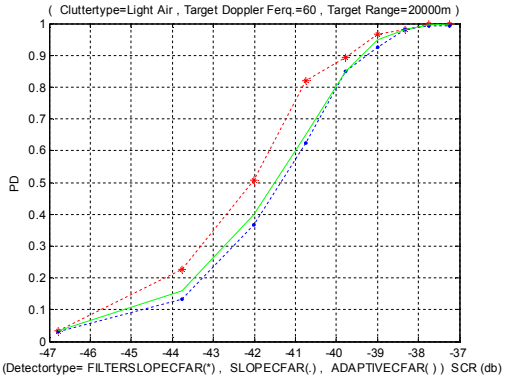

FIGURE 17. ROC Curve for second State

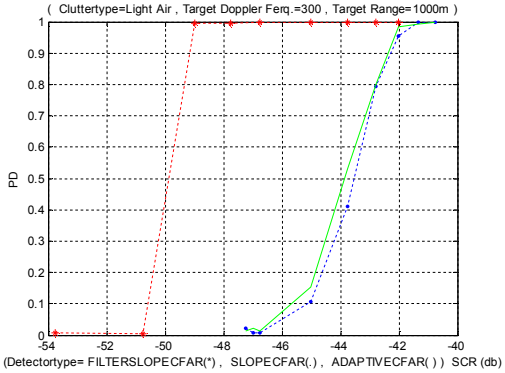

FIGURE 18. ROC Curve for Third State

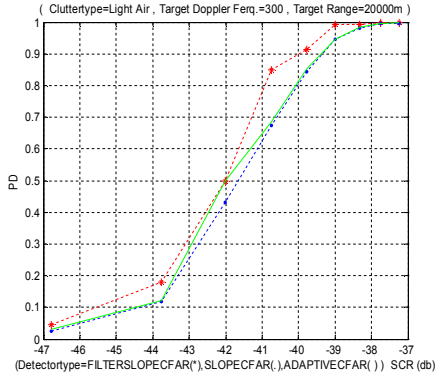

FIGURE 19. ROC Curve for 4th State

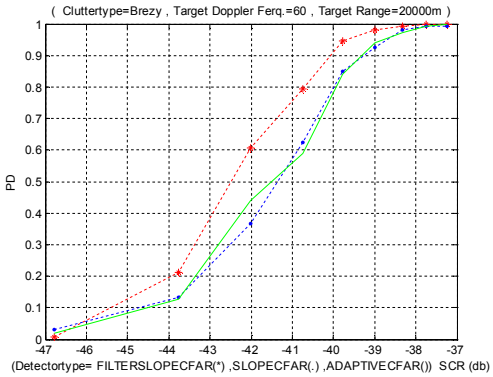

FIGURE 20. ROC Curve for 6th State

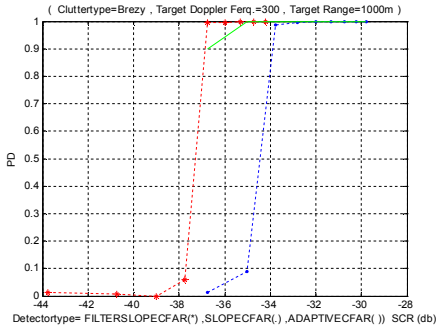

FIGURE 21. ROC Curve for 7th State

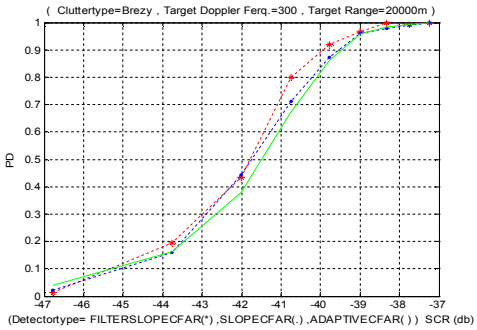

FIGURE 22. ROC Curve for 8th State

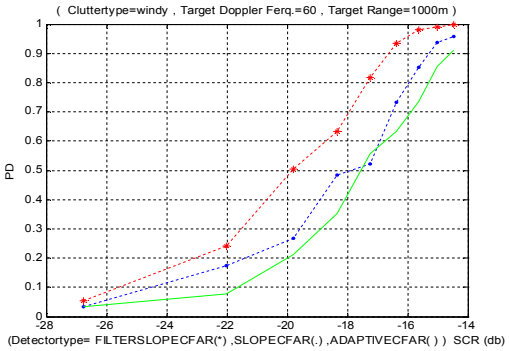

FIGURE 23. ROC Curve for 9th State

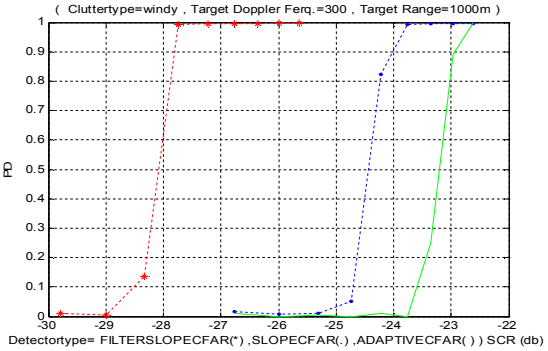

FIGURE 24. ROC Curve for 11th State

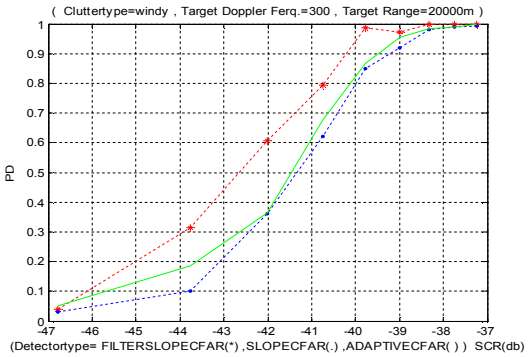

FIGURE 25. ROC Curve for 12th State

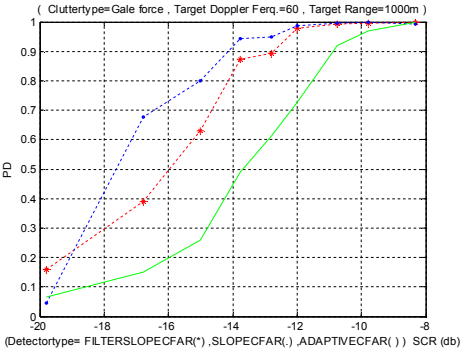

FIGURE 26. ROC Curve for 13th State

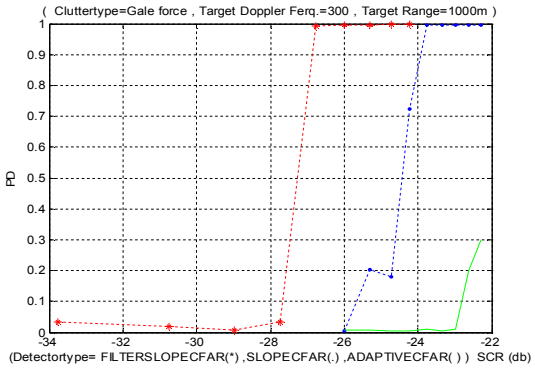

FIGURE 27. ROC Curve for 15th State

CONCLUSIONS

The aim of this paper has been to provide an overview of non-parametric and parametric spectral estimation techniques for ground surveillance pulse Doppler radar due to clutter suppression. The main difference between aforementioned techniques is the fact that in parametric techniques, a model should be supposed for the signal spectrum contemplating signal nature, but non-parametric spectral estimation techniques neglect intrinsic properties of the signal. Methods presented in the paper are simulated through computer for 4 wind conditions and two target locations (i.e. far from radar and near to it). In addition, simulation results are presented in detail. Non-parametric spectral estimation techniques (i.e. slope CFAR, filter CFAR and filter slope CFAR), and parametric techniques (i.e. AR-CFAR and AR-Yule-Walker) are investigated. The principle of each algorithm has been explained using block diagrams. Moreover, a combination of parametric and non-parametric techniques is proposed and simulated. In order to attain combination of two main techniques, clutter spectrum has been estimated by using AR model and Yule-walker method and signal spectrum is estimated by FFT based non-parametric techniques. It is concluded that a subtraction of these two spectrums yields received target echo spectrum. Finally three wind conditions are simulated and curves of PD (i.e. Probability of detection), have been illustrated with respect to SCR. Survey of simulation results proves that filter slope CFAR has the best performance and is the best approach between algorithms which has been suggested in this paper.

REFERENCES

1. Broersen. P. M. T, Wensink. H. E, 1993, On Finite Sample Theory for Autoregressive Model Order Selection, IEEE Transactions on Signal Processing, Vol. 41, No. 1,pp. 194-204.
2. Li.H, 2010, Analysis of Parametric Adaptive Signal Detection with Application To Radars And Hyper Spectral Imaging, Stevens Institute of Technology, Department of Electrical and Computer Engineering, No. A163715, pp: 138.
3. Hong. H. E, Fang. L. I. U, Zhang. B. F , Tian. Y, Wang. K. X, Hui. M, HOU.M.F, 2009 , Simulation For Doppler Signal Periodogram Spectral Estimation Method, Tianjin University of Technology, IEEE, Piezoelectricity, Acoustic Waves, and Device Applications (SPAWDA) and 2009 China Symposium on Frequency Control, Joint Conference of the 2009 Symposium on Technology, pp:67.
4. Peltier. J.T, September 1989, A Study Of Ground Clutter Suppression At The Chill Doppler Weather Radar, National Science Foundation Grant ATM 83-20095 Champaign, Illinois.
5. Sheikhi. A, 2002, Radar Target Detection in Ground Surveillance Radars, Technical report, School of Engineering, Shiraz University, Iran, No. 79-EN-1315-657.
6. Nitzberg. R, 1972, Constant-False-Alarm-Rate Signal Processors for Several Types of Interference, Syracuse, IEEE Transaction on aerospace and electronic systems, VOL. AES-8, No. 1, pp.27-34.
7. E. Davila .C, 1998, A Subspace Approach to Estimation of Autoregressive Parameters From Noisy Measurements, Electrical Engineering Department, Southern Methodist University Dallas, IEEE Transactions on Signal Processing, Vol. 46, No. 2, pp. 531-534.
8. Sakae. C, keiichi. S, Matso. S, Toshimitsu. M, 1991, Suppression of Radar Clutter via Nonparametric CFAR, Electronic and Communications in Japan, Part 1, Tokyo Institute of Technology, Yokohama, Japan, Vol 74, No. 6, pp. 107-114.
9. Bezerra. M. I. S, Iano. Y, Tarumoto. M. H, 2008, Evaluating some Yule-Walker Methods with the Maximum-Likelihood Estimator for the Spectral ARMA Model, TEMA Tend. Mat. Apl. No. 2 ,pp:175-184.
10. Oktay. A, 1988,Study of Model-Order Selection Algorithms And Their Applicability to Adaptive Clutter Suppression, Southern Illinois University at Edwardsville Department of Electrical Engineering, Edwardsville, Conference proceeding southeastcon'88, IEEE, pp: 55-60.
11. Bing .D, Ran .T, Lu .M, 2006, Novel Long-Term Coherent Integration Method for Moving-Target-Detection, Dept. of Electron. Eng. Beijing Inst. of Technol, International Conference on RadarCIE'06, IEEE, No. 0-7803-9582-4, pp: 1266-1268.
12. De HoonM. J. L. , Van Der Hagen T.H.J.J , Schoonewelle .H, Van Dam .H, October 1996, Why Yule-Walker should not be used for autoregressive modeling, Interfaculty Reactor Institute, Delft University of Technology Mekelweg 15, 2629 JB Delft, The Netherlands, Annals of Nuclear Energy, Vol 23, No. 15, pp: 1219-1228.